Observation of ρ/ω Meson Modification in Nuclear Matter

K. Ozawa,* H. En'yo, H. Funahashi, M. Kitaguchi, M. Ishino,† H. Kanda,‡ S. Mihara,† T. Miyashita,§ T. Murakami, R. Muto, M. Naruki, F. Sakuma, H. D. Sato, T. Tabaru, S. Yamada, S. Yokkaichi,‖ and Y. Yoshimura¶
Department of Physics, Kyoto University, Kitashirakawa Sakyo-Ku, Kyoto 606-8502, Japan

J. Chiba, M. Ieiri, M. Nomachi,** O. Sasaki, M. Sekimoto, and K. H. Tanaka
Institute of Particle and Nuclear Studies, KEK, 1-1 Oho, Tsukuba, Ibaraki 305-0801, Japan

H. Hamagaki
Center for Nuclear Study, Graduate School of Science, University of Tokyo, 7-3-1 Hongo, Tokyo 113-0033, Japan
(Received 14 November 2000)

We measured the invariant mass spectra of electron-positron pairs in the target rapidity region of 12-GeV $p + A$ reactions. We have observed a significant difference in the mass spectra below the ω meson between p + C and p + Cu interactions. This difference indicates that the spectral shape of mesons is modified at normal nuclear-matter density.

DOI: 10.1103/PhysRevLett.86.5019 PACS numbers: 25.40.Ve, 14.40.Aq, 21.65.+f, 24.85.+p

Recently, the chiral property of QCD in hot ($T \neq 0$) or dense ($\rho \neq 0$) nuclear matter has attracted wide interest in the field of hadron physics. The dynamical breaking of chiral symmetry in the QCD vacuum induces an effective mass of quarks, known as constituent quark mass, which then determines the known mass of all the hadrons. In hot and/or dense matter, this broken symmetry is subject to be restored either partially or completely and, hence, the properties of hadrons can be modified. To observe such an effect, measurements of the in-medium decay of vector mesons are highly desirable for the direct determination of the meson properties in matter.

Although many heavy-ion experiments have been carried out in CERN-SPS and BNL-AGS to study hot and dense matter, only one experiment could address the mass modification of vector mesons. The CERES/NA45 Collaboration measured low-mass electron-pair productions in Pb-Au collisions at 158 A GeV [1], and observed an enhancement of the e^+e^- pair yield in the mass range of $0.3 < m_{ee} < 0.7$ GeV/c^2 over the expected yield from the known hadronic sources in pp collisions. This striking effect could be understood as a consequence of the mass modification of a ρ and a ω meson in hot matter.

On the other hand as an interpretation of K^+-^{12}C scattering data [2], Brown *et al.* proposed a possible modification of the ρ meson mass at normal nuclear density. After this suggestive but an indirect information, the TAGX Collaboration reported the direct observation of a modified ρ meson in $\pi^+\pi^-$ invariant mass spectra in the $^3\mathrm{He}(\gamma, \pi^+\pi^-)X$ channel [3]. Further experimental data, especially regarding the lepton channel which is free from the effect of final state interactions, are awaited, since the TAGX data were based on subthreshold ρ meson production and not free from the influence of the limited phase space.

There are several theoretical approaches to the investigation of meson modification and its density dependence [4,5]. For example, one model based on the QCD sum rule has been proposed by Hatsuda and Lee [4]. According to this model, the mass decrease at normal nuclear density is $\sim$120–180 MeV/c^2 for the ρ and ω mesons and $\sim$20–40 MeV/c^2 for the ϕ meson. Brown and Rho proposed another scaling law which predicts that the masses of ρ and ω mesons decrease 20% at normal nuclear density [5]. Thus, the measurements of such mesons, which are produced and decayed in a nucleus, are of great interest. The present experiment is one of several experimental efforts [6] to investigate the in-medium properties of the vector mesons at normal nuclear-matter density.

The experiment, KEK-PS E325, was designed to measure the decays of the vector mesons, $\phi \rightarrow e^+e^-$, $\rho/\omega \rightarrow e^+e^-$, and $\phi \rightarrow K^+K^-$, in the kinematical region where the decay probability inside a target nucleus was enhanced ($0.6 < \text{rapidity}_{ee} < 2.2$, $0.0 < P_{Tee} < 1.5$ GeV/c). Considering the observed kinematical distributions, it is expected that about 60% of ρ mesons and about 10% of ω mesons decay statistically inside a copper nucleus if no mass broadening takes place in the nuclear medium. This rate increases according to the width broadening in the nucleus. We thus expect to see a "free-space" peak consisting of mesons decayed outside the nucleus. And the effect of meson modification could be seen as an excess over the known spectra.

The spectrometer was built at the primary beam line EP1B in the 12GeV-PS at KEK. We have been taking data since 1998. This report describes the e^+e^- triggered data of 5.6×10^7 events collected in 1998 using 2.2×10^{14} protons on the targets. The layout of the detectors is shown in Fig. 1. The spectrometer had two electron arms and two kaon arms, which shared the dipole magnet and the tracking devices. The electron arms covered $\pm 12°$ to $\pm 90°$ horizontally and $\pm 22°$ vertically. The kaon arms covered $\pm 12°$ to $\pm 54°$ horizontally and $\pm 6°$ vertically. Primary protons with a typical intensity of 7×10^8 Hz

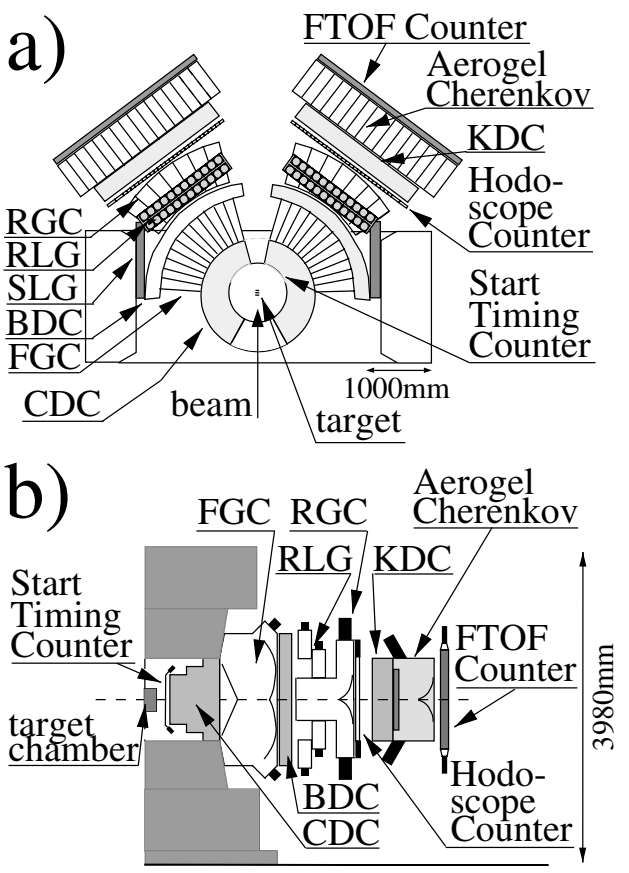

FIG. 1. Schematic view of the experimental setup of the E325 spectrometer: (a) the top view and (b) the side view. The side view shows the cross section along the center of the kaon arm (see text).

were delivered to the targets at the center of the dipole magnet. We used three kinds of targets (carbon, polyethylene, and copper) aligned in-line with interaction lengths of 0.028%, 0.061%, and 0.020%, respectively. The carbon and copper targets were glued onto target supports made of paper ($C_6H_{12}O_6$), whose interaction length was 0.033%. The combination of an intense beam with a thin target was essential to keep the γ conversion rate below the Dalitz decay rate. The typical interaction rate was as high as 1.2 MHz. The three targets were separated by 40 mm, and the target images were reconstructed by the charged tracks with 4.2 mm resolution in the beam direction.

Tracking was performed using a cylindrical drift chamber (CDC) and barrel-shaped drift chambers (BDC). The dipole magnet had circular pole pieces of 880 mm in radius. The magnet provided the field of 0.78 T at the center, and the field integral of 0.81 Tm from the center to 1600 mm in radius where the BDC's were located. The acceptance of the CDC was $\pm 12°$ to $\pm 132°$ horizontally and $\pm 22°$ vertically, while the BDC had the same vertical coverage as the CDC with a smaller horizontal coverage of $\pm 7.5°$ to $\pm 94.5°$. The CDC consisted of ten layers of the drift cells in the radial region of 445.0 to 830.0 mm including four stereo layers. The BDC's had four layers, located in the radial region of 1600 to 1650 mm, including two stereo layers. All of the drift cells of the CDC had the same horizontal angular coverage of 1.5° with respect to the target, and the drift cells of the BDC had an angular coverage of 0.75°. Both the CDC and BDC used argon-ethane mixed gas of 50% and 50% at 1 atm. The total thickness of the materials from the target to the front of the BDC was 3.1% of the radiation length. A position resolution of 350 μm was obtained in the present analysis.

For electron identification, the whole region of the electron arm was covered by two stages of electron-identification counters. The first stage of electron identification was performed by the front gas-Čerenkov counters (FGC), which covered from $\pm 12°$ to $\pm 90°$ horizontally and $\pm 22°$ vertically. They were horizontally segmented into 13 units in each arm so that one segment covered 6°. The second stage consisted of three types of electron-identification counters. The rear gas-Čerenkov counters (RGC) covered $\pm 12°$ to $\pm 54°$ horizontally and $\pm 6°$ vertically with seven horizontal segments in each arm. These regions corresponded to the kaon-arm acceptance. The rear lead-glass electromagnetic (EM) calorimeters (RLG) covered the same horizontal angle as the RGCs with 12 segments in each arm, but were vertically covered outside the kaon-arm acceptance, from $\pm 6°$ to $\pm 22°$. In the backward region, where the horizontal angle was larger than 57°, the second-stage electron identification was performed by side lead-glass EM calorimeters (SLG) which covered $\pm 57°$ to $\pm 90°$ horizontally and $\pm 22°$ vertically with nine horizontal segments in each arm.

Both of the gas-Čerenkov counters used isobutane with a refractive index of 1.0019. The threshold momentum for pions was 2.3 GeV/c. Both the RLG and the SLG consisted of SF6W lead glass. The typical energy resolution of the RLG and the SLG was $15\%/\sqrt{E}$. To suppress any fake triggers caused by pions and protons, we set the discriminater threshold for the gas-Čerenkov counters higher than the optimum setting for electrons; thus, the electron efficiency was sacrificed. For electrons with a momentum greater than 400 MeV/c, the overall efficiencies, including the trigger threshold and the off-line cut, were 55% for FGC, 86% for RGC, and 85% for the calorimeters, RLG and SLG. We achieved a pion rejection of 6.7×10^{-4} using a cascade operation of FGC and the EM calorimeters, and 3.9×10^{-4} with FGC and RGC for 400 MeV/c pions.

An electron trigger having three levels was adopted to perform the data accumulation. In the first level, we selected electron-pair candidates using the coincidence signals of the front-stage (FGC) and the rear-stage detectors (SLG, RLG, RGC), by requiring horizontal position matching. To suppress electron pairs having small opening angles, such as from Dalitz decays and γ conversions, we required the two FGC hits to be more than two segmentations apart. In the second level, we required the pair to be oppositely charged by using the drift-chamber hits associated with the FGC hits. The sign

of a track can be roughly determined by hits in the outermost layers in the CDC and in the BDC together with the target position. We eliminated the electron-pair candidates which had an apparent "++" or "−−" configuration. We also required the remaining pairs to be more than 12° apart at the $r = 825$ mm position in order to suppress electron pairs having small opening angles. In the third level, the approximate opening angles of the pairs were calculated. Because the radius of the BDC layers was almost twice that of the radius of the outermost CDC layers, the opening angle of the pair at the target, Θ_{open}, could be approximated by $\Theta_{\text{open}} \simeq 2 \times \Theta_{\text{cdc}} - \Theta_{\text{bdc}}$, where Θ_{cdc} is the opening angle of the pair at the outermost CDC layer and Θ_{bdc} at the BDC layer with respect to the target position. We required Θ_{open} to be in the range from 50° to 150° in the trigger. The typical trigger rates were 450, 330, and 280 Hz in the first, second, and third level triggers, respectively. We maintained the live time of the data acquisition at around 60%.

To evaluate the performance of the spectrometer, the mass resolution was examined for the observed peaks of the $\Lambda \rightarrow p + \pi^-$ and $K_s \rightarrow \pi^+ + \pi^-$ decays, as shown in Figs. 2a and 2b. For the Λ peak we obtained the centroid at 1115.5 MeV/c^2 (known to be 1115.7 MeV/c^2) with a Gaussian resolution of 1.8 ± 0.1 MeV/c^2, and for K_s 493.9 MeV/c^2 (known to be 497.7 MeV/c^2) and 3.6 ± 0.6 MeV/c^2, respectively. The observed peak positions and widths provide the systematic uncertainty of the mass scale and the mass resolution of the present analysis. The results were compared to Monte Carlo simulations in which we took the chamber resolution and the multiple scattering into account. The observed widths were well reproduced by the simulation (1.9 ± 0.6 MeV/c^2 for Λ and 3.5 ± 0.6 MeV/c^2 for K_s), and the energy scale uncertainties for the ω and ϕ mesons were estimated to be 4 and 7 MeV/c^2, and the mass resolution to be 9.6 and 12.0 MeV/c^2, respectively.

Figure 3 shows the e^+e^- invariant mass spectra: (a) for the carbon and polyethylene targets (light nuclear targets) and (b) for the copper target (heavy nuclear target). These histograms depict the events when the electron and the positron are detected in different arms, so that the low-mass part of the spectra is largely suppressed. Although the clear peaks of the ω meson decaying into e^+e^- are visible in the spectra, a significant shape difference is observed between the light nuclear targets and the copper target, and an excess at the low-mass side of the ω peak can be seen.

We tried to reproduce the mass shape of the obtained histograms using the combinatorial background and the

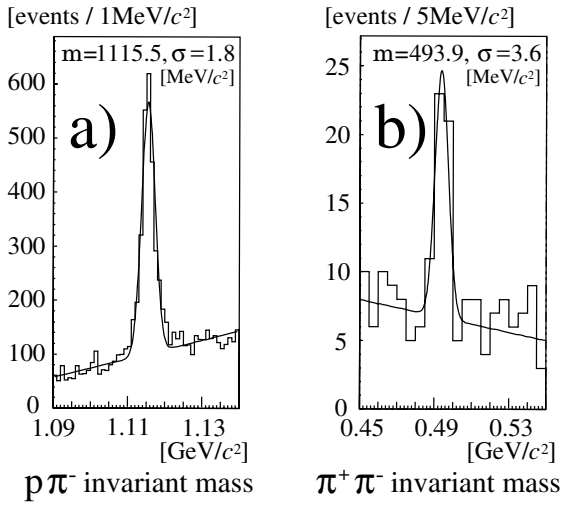

FIG. 2. Invariant mass spectrum of $p\pi^-$ (a) and $\pi^+\pi^-$ (b). The lines are the best-fit results by applying a Gaussian with a linear background.

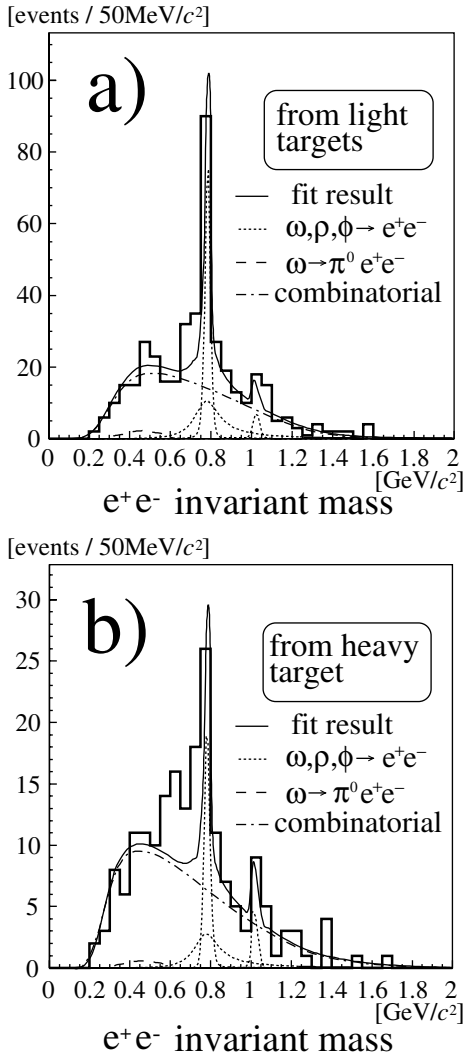

FIG. 3. Invariant mass spectrum of the e^+e^- pair: (a) for the carbon and polyethylene targets and (b) for the copper target. The solid lines show the best-fit results of the known hadronic sources with the combinatorial background. The dotted lines indicate the contributions from ρ, ω, and ϕ decays. The dashed lines indicate $\omega \rightarrow \pi^0\, e^+e^-$ decays and the dot-dashed lines indicate the combinatorial background.

known hadronic sources. The origins of the combinatorial background were pairs which were picked up from two independent Dalitz decays or γ conversions, and pairs like $e^-\pi^+$ or $e^+\pi^-$ due to misidentification. The remaining $e^-\pi^+$ and $e^+\pi^-$ background was estimated to be about 13% in the spectra and contaminations such as $\pi^+\pi^-$ to be negligibly small. The distribution of the combinatorial background was obtained using the event-mixing method. As known hadronic sources, $\rho \to e^+e^-$, $\omega \to e^+e^-$, $\phi \to e^+e^-$, $\eta \to e^+e^-\gamma$, and $\omega \to e^+e^-\pi^0$ were considered. Contributions from particles with higher masses are known to be insignificant [7]. The Dalitz decay, $\pi^0 \to e^+e^-\gamma$, is negligible in the mass acceptance of the present data. The shapes of the e^+e^- invariant mass spectra from the Dalitz decays, $\eta \to e^+e^-\gamma$ and $\omega \to e^+e^-\pi^0$, were taken from Ref. [8]. The mass shape of the ρ, ω, and ϕ mesons was given as the Breit-Wigner function with the natural widths 150, 8.41, and 4.43 MeV/c^2, respectively. The Breit-Wigner functions were smeared with the estimated mass resolutions of 9.6 MeV/c^2 for the ω and 12.0 MeV/c^2 for the ϕ meson. Because the present experiment used targets with a radiation length of less than 0.3%, the radiative tail and the multiple scattering due to the target thickness were negligible. To obtain the mass shape of the known sources in the observed spectra, we evaluated the experimental mass acceptance using the particle distributions obtained by the nuclear cascade code, JAM [9], which reproduced the rapidity and P_t spectra of the observed e^+e^- pairs.

The relative abundances of the known sources and the combinatorial background were obtained through fitting with four parameters, the amplitudes of $\rho/\omega \to e^+e^-$, $\phi \to e^+e^-$, $\eta \to \gamma e^+e^-$, and the combinatorial background. We assumed that the production cross section of ρ is equal to that of ω following the data obtained at the same energy [10]. The amplitude of the other source, $\omega \to \pi^0 e^+e^-$, was given by the branching ratio. The best fits are overplotted in Fig. 3. As a result of the fits, the contribution of $\eta \to \gamma e^+e^-$ turned out to be negligible, and we found 75.5 $\pm$ 9.0 ω mesons and 7.4 $\pm$ 5.8 ϕ mesons from the light target and 20.0 $\pm$ 4.8 ω mesons and 5.2 $\pm$ 2.7 ϕ mesons from the copper target. The invariant mass shapes were well reproduced, except for the mass region below the omega peak.

To evaluate the excess, we would like to avoid introducing "modified" spectra which are not reliably predictable. We thus repeated the same fit procedure excluding the mass region from 550 to 750 MeV/c^2, where the excess is visible. The excess was estimated by subtracting the amplitude of the fit function from the data. The amount of the excess of the light target was 19.6 $\pm$ 11.7 and that of the copper target was 29.5 $\pm$ 8.7. The excess is statistically significant for the copper target data. The ratios to the amplitude of the ω peak are 0.26 $\pm$ 0.16 for the light target and 1.48 $\pm$ 0.56 for the copper target. The difference between the two cases should have originated from the difference in the nuclear size. The relative yields of the ρ/ω meson for both targets *including* the excess follow $A^{0.67\pm0.12}$, being consistent with $A^{2/3}$ [11], where A is the nuclear mass number.

A natural explanation for the shape change is that the spectral modification of ρ/ω mesons takes place inside a nucleus. Although the spectra of the modified meson is difficult to predict, it should be noted that the excess in the copper target data is visible in the mass range of about 200 MeV below the ω peak.

In summary, we have observed a significant difference in the e^+e^- invariant mass spectra around the ρ/ω region between carbon and copper targets, which indicates that the spectral shapes of mesons are modified at normal nuclear-matter density.

We would like to thank all of the staff members of KEK-PS, especially the beam channel group for their helpful support. This work was partly funded by the Japan Society for the Promotion of Science and a Grant-in-Aid for Scientific Research from the Ministry of Education, Science, and Culture of Japan (Monbusho).

*Present address: Center for Nuclear Study, Graduate School of Science, University of Tokyo, 7-3-1 Hongo, Tokyo 113-0033, Japan.
Email address: ozawa@cns.s.u-tokyo.ac.jp
†Present address: ICEPP, University of Tokyo, 7-3-1 Hongo, Tokyo 113-0033, Japan.
‡Present address: Physics Department, Graduate School of Science, Tohoku University, Sendai 980-8578, Japan.
§Present address: Fujitsu Corporation, 4-1-1, Kamikodanaka, Nakahara, Kawasaki, Kanagawa 211-8588, Japan.
‖Present address: RIKEN, 2-1 Hirosawa, Wako, Saitama 351-0198, Japan.
¶Present address: Xaxon Corporation, 1-3-19, Tanimachi, Chu-ou, Osaka, Japan.
**Present address: Department of Physics, Osaka University, 1-1 Machikaneyama, Toyonaka, Osaka 560-0043, Japan.

[1] G. Agakichiev *et al.,* Phys. Lett. B **422**, 405 (1998).
[2] G. E. Brown *et al.,* Phys. Rev. Lett. **60**, 2723 (1988).
[3] G. J. Lolos *et al.,* Phys. Rev. Lett. **80**, 241 (1998); M. A. Kagarlis *et al.,* Phys. Rev. C **60**, 025203 (1999).
[4] T. Hatsuda and S. H. Lee, Phys. Rev. C **46**, R24 (1992).
[5] G. E. Brown and M. Rho, Phys. Rev. Lett. **66**, 2720 (1991).
[6] HADES Collaboration, W. Schoen *et al.,* Acta Phys. Pol. B **27**, 2959–2963 (1996). GSI/SIS proposal S214, Search for bound η- and ω-nuclear states using the recoilless $(d, {}^3\mathrm{He})$ reaction. T. Nakano *et al.,* Nucl. Phys. **A629**, 559c (1998). KEK-PS E325 proposal (http://www.pn.scphys.kyoto-u.ac.jp/phi/E325_project.html).
[7] T. Akesson *et al.,* Z. Phys. C **68**, 47 (1995).
[8] A. Faessler, C. Fuchs, and M. I. Krivoruchenko, Phys. Rev. C **61**, 035206 (2000).
[9] Y. Nara *et al.,* Phys. Rev. C **61**, 024901 (1999).
[10] V. Blobel *et al.,* Phys. Lett. **48B**, 73 (1974).
[11] M. Binkley *et al.,* Phys. Rev. Lett. **37**, 571 (1976).